

## INTERACTION OF SYNTHETIC SULPHATE “GREEN RUST” WITH PHOSPHATE AND THE CRYSTALLIZATION OF VIVIANITE

HANS CHRISTIAN BRUUN HANSEN AND INGE FIIL POULSEN

Chemistry Department, Royal Veterinary and Agricultural University,  
Thorvaldsensvej 40, DK-1871 Frdb. C, Copenhagen, Denmark

**Abstract**—Because layered Fe(II)Fe(III)-hydroxides (Green rusts, GRs) are anion exchangers, they represent potential orthophosphate sorbents in anoxic soils and sediments. To evaluate this possibility, two types of experiments with synthetic sulphate-interlayered GRs ( $\text{GR}_{\text{SO}_4} = \text{Fe}^{2+}_4\text{Fe}^{3+}_2(\text{OH})_{12}\text{SO}_4 \cdot x\text{H}_2\text{O}$ ) were studied. First, sorption of phosphate in  $\text{GR}_{\text{SO}_4}$  was followed by reacting suspensions of pure  $\text{GR}_{\text{SO}_4}$  synthesized by oxidation of Fe(II) with an excess of  $\text{Na}_2\text{HPO}_4$  (pH 9.3). Second the possible incorporation of phosphate in GR during formation by Fe(II)-induced reductive dissolution of phosphate-containing ferrihydrites was examined in systems containing an excess of Fe(II) (pH 7). With excess phosphate in solution,  $\text{GR}_{\text{SO}_4}$  initially sorbed phosphate in the interlayer producing a basal layer spacing of 1.04 nm, but only ~50% of the interlayer sulphate was exchanged with phosphate. This GR slowly transformed to vivianite within months. In the Fe(II)-rich systems, reaction with synthetic ferrihydrites produced  $\text{GR}_{\text{SO}_4}$  similar to that produced by air oxidation. Reaction of Fe(II) with phosphate-containing ferrihydrites initially produced amorphous greenish phosphate containing precipitates which, after 3–4 h, crystallized to  $\text{GR}_{\text{SO}_4}$  and vivianite. In these solutions, stable phosphate-free  $\text{GR}_{\text{SO}_4}$  can form since precipitation of vivianite produced low phosphate activity. Consequently, in both systems GR or amorphous greenish precipitates act as reactive intermediates, but vivianite is the stable end-product limiting phosphate concentration in solution. It is also inferred that  $\text{Fe}(\text{OH})_2$  is an unlikely phosphate sorbent in mixed Fe(II)-Fe(III) systems because GR phases are more stable (less soluble) than  $\text{Fe}(\text{OH})_2$ .

**Key Words**—Anion Exchange, Fe(II)Fe(III)-hydroxides, Green Rust, Layered Hydroxides, Phosphate, Vivianite.

### INTRODUCTION

The mechanisms causing retention of phosphate in anoxic soils and sediments are not well understood. Under anaerobic conditions, microbial activity may lead to the reductive dissolution of iron(III)(hydr)oxides (Lovley, 1987) that will result in mobilization of phosphate adsorbed to the iron(III)(hydr)oxides. This process will cause an increase in phosphate concentration in the soil solution (Ponnamperuma, 1972; Willett, 1986, 1989; Lovley, 1991; Szilas *et al.*, 1997). In neutral anaerobic environments, phosphate concentrations can often stabilize at levels that are not much higher than in aerobic soils. Several workers have suggested Fe(II)-hydroxide or mixed Fe(II)Fe(III)-hydroxides as the active phosphate sorbents in anoxic soils and sediments (Williams *et al.*, 1971; Patrick and Khalid, 1974; Willett and Higgins, 1978; Holford and Patrick, 1979). Retention of P due to precipitation of Fe(II)-phosphates like vivianite is another possibility (Nriagu and Dell, 1974; Willett, 1985).

Green rusts (GRs) represent Fe(II)Fe(III)-hydroxides, which can form in anoxic environments (Taylor, 1980; Hansen *et al.*, 1994) and GR-like compounds have recently been identified in gley soils (Trolard *et al.*, 1997). GRs belong to the pyroaurite-class of layered double metal hydroxides, LDHs (Bernal *et al.*, 1959; Brindley and Bish, 1976). These compounds have the ideal composition  $[\text{Fe}^{2+}_{(6-x)}\text{Fe}^{3+}_x(\text{OH})_{12}][(\text{A}_{x/n})_n \cdot y\text{H}_2\text{O}]$ , where  $\text{A}^{n-}$

is an n-valent exchangeable anion placed in the interlayer between planar trioctahedral Fe(II)Fe(III)-hydroxide layers (Allmann, 1970). Many synthesis routes have been proposed to explain the formation of GR, two methods seem most relevant to natural environments. The first method is comprised of the Fe(II)-mediated dissolution of ferrihydrite or lepidocrocite at constant pH ( $\geq 7$ ) with concurrent precipitation of GR (Taylor and McKenzie, 1980; Tamaura *et al.*, 1984a). In the other method, GRs precipitate when Fe(II) salt solutions are partly oxidized by  $\text{O}_2$  at constant pH (Feitknecht and Keller, 1950; Tamaura *et al.*, 1984b; Vins *et al.*, 1987). If, besides  $\text{OH}^-$ , only the anion of the particular Fe(II) salt is present, this anion is incorporated in the GR-interlayer.

Green rusts have high potential anion exchange capacities and may be expected to show considerable affinity for bonding of di- or trivalent phosphate anions. High affinity and capacity for adsorption of phosphate was observed for hydrotalcite, a Mg-Al-analogue of GR (Hansen, 1995; Shin *et al.*, 1996). Precipitating hydrotalcite and analogue LDHs as scavengers of environmentally harmful oxyanions was demonstrated by Reardon and Della Valle (1997).

The major objectives of this paper are to report on two possible mechanisms for phosphate retention by sulphate green rust ( $\text{GR}_{\text{SO}_4}$ ), which may commonly occur in hydromorphic natural systems. Two types of experiments were employed to investigate the phos-

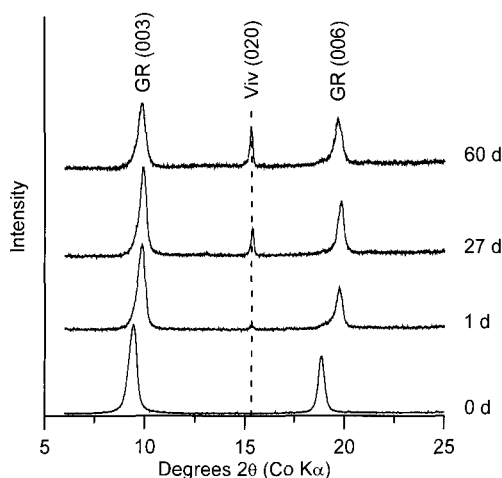


Figure 1. Basal reflections of  $GR_{SO_4}$  and 020 reflection of vivianite (Viv) precipitated after reacting 2.5 mM of  $GR_{SO_4}$  with 20 mM  $NaHPO_4$  for different periods of time. (Indices refer to a hexagonal cell for GR and a monoclinic cell for Viv.)

phosphate-sorbing role of  $GR_{SO_4}$ : (1) Reaction of  $GR_{SO_4}$  with phosphate-rich solutions, and (2) Reductive dissolution of phosphate containing ferrihydrite in the presence of excess Fe(II) during the formation of  $GR_{SO_4}$ .

## MATERIALS AND METHODS

### Synthesis of $GR_{SO_4}$ and reaction with $Na_2HPO_4$

The  $GR_{SO_4}$  was synthesized by air oxidation of  $FeSO_4$  solutions at pH 7 (Koch and Hansen, 1997). Ten milliliters of a 500 mM Fe(II) salt solution under Ar (99.999%, 60 ml·min<sup>-1</sup>) was oxidized at a rate resulting in a base consumption of  $7 \times 10^{-7}$  mol·s<sup>-1</sup> until oxidation of ~30% of the initial Fe(II) was obtained. A pH-stat reactor was used to maintain constant pH (Hansen, 1994). The solid products were separated on a glass filter (pore diameter 10–16 μm), washed with  $6 \times 10$  ml Ar bubbled water in a glove box, divided into two 100 ml crimp-cap vials, and redispersed in 50 ml or 80 ml (blank) Ar-bubbled water. After sealing with teflon-coated rubber-septa, the vials were removed from the glovebox. One vial in a set was used as a blank; 28 ml of an Ar-bubbled 50 mM  $Na_2HPO_4$  solution (pH 9.3) was introduced to the other vial using an Ar-flushed hypodermic syringe. The flasks were wrapped in Al foil to prevent photochemical side reactions and placed on a shaking table (50 strokes·min<sup>-1</sup>) at room temperature.

For a period of 60 d, samples of the suspensions were taken for determination of Fe(II),  $SO_4^{2-}$  and phosphate concentrations and also for X-ray diffraction (XRD) analysis of solids. Samples were withdrawn using Ar-flushed hypodermic syringes. For each sampling, 1 ml aliquots of the suspensions were trans-

ferred into 20 ml of 0.1 M HCl to dissolve Fe(II)-containing solid phases, shaken for 30 min, passed through a 0.22 μm Millipore filter, and the filtrate was analyzed for Fe(II) ( $Fe(II)_{tot}$ ). Another 1 ml aliquot of the suspension was passed through a 0.22 μm Millipore filter and the filtrate was analyzed for Fe(II) and  $SO_4^{2-}$  concentrations in solution ( $[Fe(II)]_{sol}$ ,  $[SO_4^{2-}]_{sol}$ ). The material retained on the filter was washed with 5 ml water, digested for 1 h in 15 ml 0.1 M HCl and then analyzed for iron and phosphate in the filtered digest ( $Fe_{solid}$ ,  $P_{solid}$ ). Solids for examination by XRD were collected by passing 5 ml of suspension through a 0.22 μm Millipore filter. The collected solids were preserved against oxidation by wetting with glycerol (Hansen, 1989).

### Reaction of P-ferrihydrite with Fe(II)

A reaction scheme similar to the 'induced hydrolysis' reaction of Taylor and McKenzie (1980) was used. Phosphate-containing ferrihydrite (P-ferrihydrite) was prepared by rapid neutralization of 0.05 M  $Fe_2(SO_4)_3$  + 0.075 M  $NaH_2PO_4$  with NaOH to pH 7. On average, the added P-ferrihydrite suspensions contained 0.89 mmol Fe(III), 0.67 mmol P, and 2.55 mmol NaOH. This suspension was added to 200 ml of a 25 mM solution of Mohr's salt ( $(NH_4)_2Fe(SO_4)_2 \cdot 6H_2O$ ) in a pH-stat reactor flushed with Ar. The pH was controlled at 7.0 using 0.5 M NaOH as titrant. For comparison, the same amounts of pure ferrihydrites (precipitated as described above, but without addition of phosphate) were reacted under similar conditions. During reaction, samples were withdrawn for determination of  $Fe(II)_{sol}$ ,  $Fe(II)_{tot}$ , and for XRD.

### Analytical procedures

Iron(II) was determined by the 1,10-phenanthroline method (Fadrus and Maly, 1975). Total iron was determined similarly, but after prior reduction with hydroxylamine (10% (weight/volume)). Sulphate was determined by capillary electrophoresis (Westergaard *et al.*, 1998), and phosphate by a molybdate-blue method adapted to flow injection analysis (Tecator, 1983). Calculation of equilibrium concentrations used the code MINTEQA2 (Allison *et al.*, 1990). XRD patterns of the GR-glycerol samples smeared on  $4 \times 4$  cm glass plates were recorded using a Philips PW1050 goniometer applying Fe-filtered  $CoK\alpha$  radiation and a scanning speed of 1 °2θ·min<sup>-1</sup>. X-ray scan data were processed using the Siemens DiffracPlus software, ver. 2.2 (Siemens, 1997).

## RESULTS

### Reaction of $GR_{SO_4}$ with $Na_2HPO_4$

The synthesis method resulted in pure and highly crystalline  $GR_{SO_4}$  (Figure 1), a product assigned the  $GR_{SO_4}$  composition  $Fe^{2+}_4Fe^{3+}_2(OH)_{12}SO_4$  (Hansen *et*

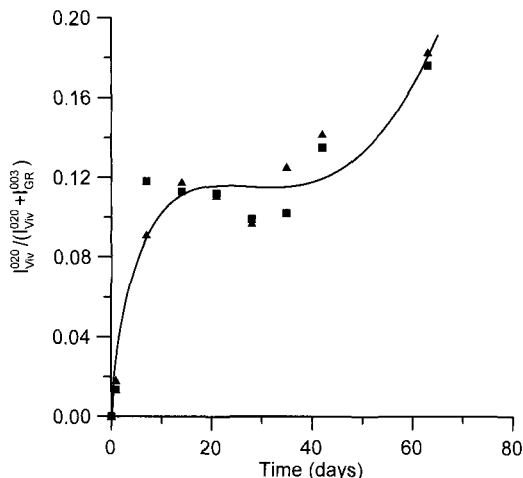


Figure 2. Rate of transformation of  $\text{GR}_{\text{SO}_4}$  into vivianite on reacting 2.5 mM  $\text{GR}_{\text{SO}_4}$  with 20 mM  $\text{Na}_2\text{HPO}_4$  represented by change in the intensity ratio  $I_{\text{Viv}}^{020}/(I_{\text{Viv}}^{020} + I_{\text{GR}}^{003})$  with time. The two symbols (▲, ■) refer to two different flasks in an experiment. (Solid line drawn for guidance, but not fitted to the data.)

*al.*, 1994, 1996). Vivianite ( $\text{Fe}_3(\text{PO}_4)_2 \cdot 8\text{H}_2\text{O}$ ) was detected within 1 d after addition of  $\text{Na}_2\text{HPO}_4$  to the  $\text{GR}_{\text{SO}_4}$  suspension; with time more vivianite formed (Figures 1 and 2). The rate of vivianite formation was determined by measuring the intensity ratio  $I_{\text{Viv}}^{020}/(I_{\text{Viv}}^{020} + I_{\text{GR}}^{003})$  vs. time, where  $I_{\text{Viv}}^{020}$  is the integrated intensity of the 020 vivianite reflection and  $I_{\text{GR}}^{003}$  the integrated intensity of the 003 GR reflection (Figure 2). The formation rate of vivianite was initially fast (to 10 d), then ceased during a period of  $\sim 20$  d after which crystallization again took place. As determined from the intensity ratios,  $<30\%$  of the GR was converted to vivianite during the 60 d period.

The freshly synthesized  $\text{GR}_{\text{SO}_4}$  has a  $d(003)$ -value of 1.086 nm; on reaction with  $\text{Na}_2\text{HPO}_4$  this spacing decreases by 0.042 nm. A similar decrease in interlayer thickness was not observed in  $\text{GR}_{\text{SO}_4}$  suspensions without  $\text{Na}_2\text{HPO}_4$  (Figure 3). Consequently, the change in interlayer thickness is attributed to the phosphate treatment. The  $\text{GR}_{\text{SO}_4}$  remained well-crystalline in both the phosphate and control experiments during the 60 d period ( $W_{\text{HH}} = 0.396 \pm 0.024 \text{ } ^\circ 2\theta$ ). The crystallized vivianite was also highly crystalline ( $W_{\text{HH}} = 0.189 \pm 0.021 \text{ } ^\circ 2\theta$ ).

In both the phosphate-rich and control experiments the concentration of  $\text{Fe}(\text{II})_{\text{tot}}$  remained relatively constant (Figure 4). Unfortunately, it was difficult to sample the suspension reproducibly, which may explain the spread in values of  $\text{Fe}(\text{II})_{\text{tot}}$ . Less than 15% of the total  $\text{Fe}(\text{II})$  was oxidized during the 60 d period, indicating that little  $\text{O}_2$  leaked into the suspensions. The concentration of  $\text{Fe}(\text{II})_{\text{sol}}$  dropped below the detection limit after the addition of phosphate as a result of the precipitation of  $\text{Fe}(\text{II})$  phosphates (Figure 4). With

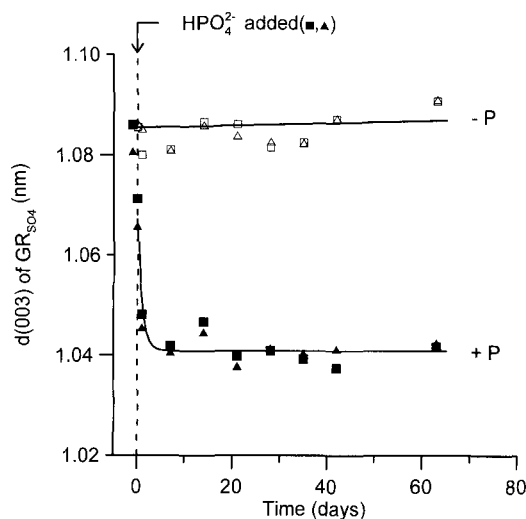


Figure 3. Comparison of the change in the  $d(003)$ -value with time for the  $\text{GR}_{\text{SO}_4}$  treated with 20 mM  $\text{NaH}_2\text{PO}_4$  (+P: ▲, ■) and for the untreated  $\text{GR}_{\text{SO}_4}$  (-P: △, □). The two symbols in a treatment refer to two different flasks in an experiment. (Solid lines drawn for guidance, but not fitted to the data.)

time, the ratio  $\text{P}_{\text{solid}}/\text{Fe}_{\text{solid}}$  decreased from 0.15 to  $<0.1$ . In test experiments, vivianite did not dissolve completely during treatment with 0.1 M HCl for 1 h. The increase in  $[\text{SO}_4^{2-}]_{\text{sol}}$  caused by addition of  $\text{Na}_2\text{HPO}_4$  to the  $\text{GR}_{\text{SO}_4}$  suspension amounted to 1.6 mM (Figure 4).

#### Reaction of ferrihydrite and P-ferrihydrite with Fe(II)

The reaction of pure ferrihydrite with Fe(II) reached completion within 60 min (Figure 5). The XRD pattern

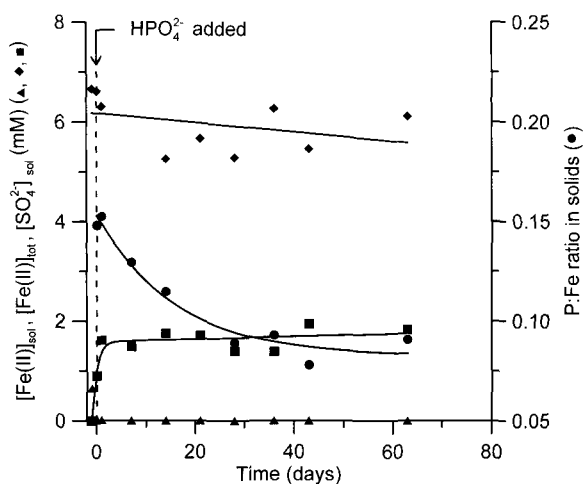


Figure 4. The change in concentration of Fe(II) in suspension ( $\text{Fe}(\text{II})_{\text{tot}}$ ), Fe(II) in solution ( $\text{Fe}(\text{II})_{\text{sol}}$ ),  $\text{SO}_4^{2-}$  in solution corrected for concentrations in blank experiments ( $[\text{SO}_4^{2-}]_{\text{sol}}$ ) and the ratio of total Fe to phosphate in the suspended solids ( $\text{Fe}_{\text{solid}}/\text{P}_{\text{solid}}$ ) with time.

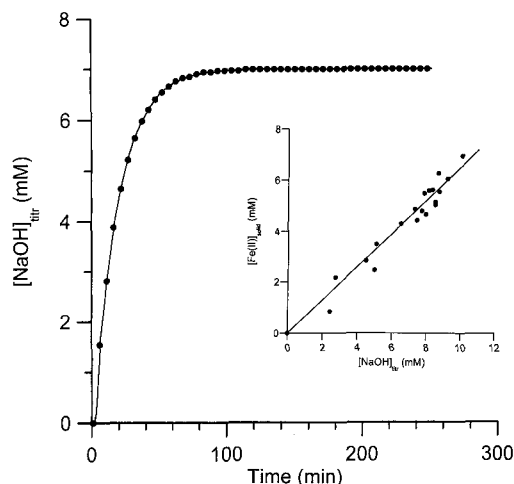


Figure 5. Typical NaOH vs. time titration curve for the reaction of 25 mM of Fe(II) with pure ferrihydrite. Insert: The consumption of NaOH per Fe(II) incorporated into  $\text{GR}_{\text{SO}_4}$  ( $[\text{Fe(II)}]_{\text{GR}}$ ). (Solid line drawn by linear regression.)

of the final product was identical to that of pure  $\text{GR}_{\text{SO}_4}$  (Figure 1). Assuming the same  $\text{GR}_{\text{SO}_4}$  composition as described above, the formation of  $\text{GR}_{\text{SO}_4}$  from ferrihydrite and Fe(II) has a theoretical consumption of 1.5 moles of  $\text{OH}^-$  per each Fe(II) incorporated into  $\text{GR}_{\text{SO}_4}$  ( $[\text{Fe(II)}]_{\text{GR}} = [\text{Fe(II)}]_{\text{tot}} - [\text{Fe(II)}]_{\text{sol}}$ ). From linear regression of  $\text{OH}^-$  consumption vs.  $[\text{Fe(II)}]_{\text{GR}}$  we determined a ratio of  $1.47 \pm 0.02$  ( $r^2 = 0.974$ ) which is in good agreement with the proposed composition of  $\text{GR}_{\text{SO}_4}$  (Figure 5, insert).

Titration curves for the reaction of soluble Fe(II) with P-ferrhydrites were completely different from those for pure ferrihydrites (Figure 5 and 6). Base consumption was initially as high as in the pure ferrihydrite system. However, after 40 min and when  $\frac{1}{3}$  of the total base was consumed, base consumption leveled off (stage I). At 200 min a new period of high-base demand started (stage II) ending with a final plateau being reached at 400–500 min (stage III). At the end of stage I only traces of GR had formed (Figure 7, trace b). During stage II more GR formed along with vivianite (Figure 7, trace c). Production of vivianite ceased at the end of stage II, where the maximum amount of GR had formed (Figure 7, trace d). The XRD patterns of the GR 003 basal spacing had a value of 1.086 nm during all stages of formation indicating that  $\text{GR}_{\text{SO}_4}$  was the form of GR present.

The consumption of  $\text{OH}^-$  titrant per Fe(II) incorporated in the crystallized solids ( $[\text{Fe(II)}]_{\text{solid}} = [\text{Fe(II)}]_{\text{tot}} - [\text{Fe(II)}]_{\text{sol}}$ ), was smaller during stage I (1.19 mol·mol $^{-1}$ , *i.e.*, 1.19 mole of  $\text{OH}^-$  per mole of Fe(II)) than stage II (1.65 mol·mol $^{-1}$ ). The approximate chemical compositions of the solid phases at different stages of reaction may be calculated from the initial compositions of the P-ferrhydrites, the data on consump-

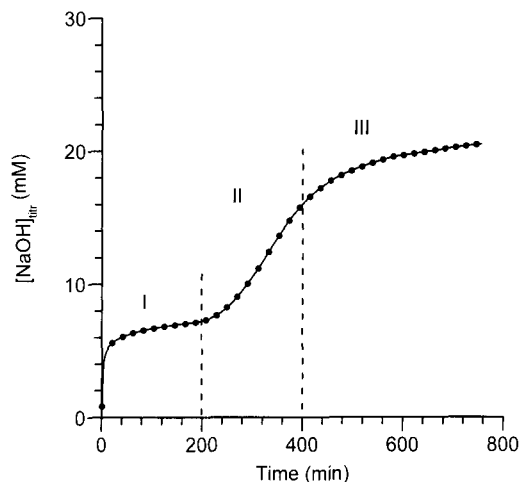


Figure 6. Typical NaOH vs. time titration curve for the reaction of Fe(II) with P-ferrhydrite.

tion of  $\text{OH}^-$  and precipitation of  $\text{Fe(II)}_{\text{solid}}$ , and the XRD data (Table 1). The precipitate formed at the end of stage I had an Fe(III):Fe(II):P:OH-ratio of 1:1.23:0.75:4.4. At the end of stage III we assume that all phosphate precipitated as vivianite, and that the residual amounts of Fe(II) and OH not present in vivianite, together with the Fe(III) from P-ferrhydrite, comprised a phase with an Fe(III):Fe(II):OH-ratio of 1:1.9:5.7. This is close to the ideal ratio for  $\text{GR}_{\text{SO}_4}$  (1:2:6), indicating that all Fe(III) in P-ferrhydrite was consumed by the production of  $\text{GR}_{\text{SO}_4}$ .

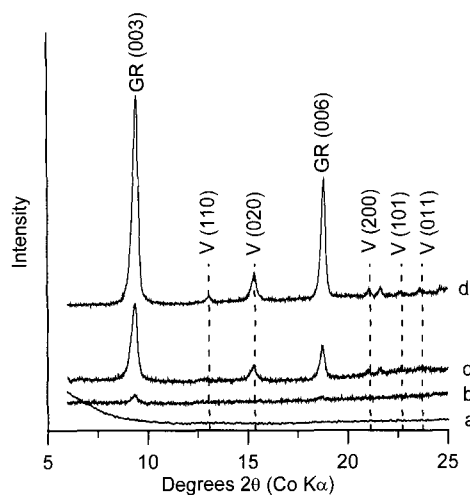


Figure 7. X-ray diffractograms of intermediates and final products in the reaction of Fe(II) with P-ferrhydrite at pH 7. (a) Initial P-ferrhydrite, (b) Product at the end of stage I, (c) Product at the middle of stage II, and (d) Final product at stage III (see Figure 6) Sample (a) was scanned as a dry powder, all other samples as glycerol smears. (GR = green rust phases, V = vivianite.)

Table 1. Average contents of Fe, P and OH in solid phases formed during reaction of Fe(II) with P-ferrhydrite.

Sample	Fe(III) (mM)	Fe(II) (mM)	H <sub>2</sub> PO <sub>4</sub> <sup>-</sup> (mM)	OH <sup>-</sup> (mM)
P-ferrhydrite <sup>1</sup>	4.4	—	3.3	12.8
End of stage I <sup>2</sup>				
Amorphous solid	4.4	5.4	3.3	19.3
End of stage III <sup>2</sup>				
Vivianite	—	4.9	3.3	6.6
GR <sub>SO<sub>4</sub></sub>	4.4	8.3	—	25.2

<sup>1</sup> Determined from the amounts of Fe<sub>2</sub>(SO<sub>4</sub>)<sub>3</sub>, NaH<sub>2</sub>PO<sub>4</sub>, and NaOH used in precipitation of this phase.

<sup>2</sup> Content determined from measurements of Fe(II)<sub>solid</sub> and consumption of NaOH (example in Figure 6). All phosphate assumed to be present in vivianite and all Fe(III) to be present in GR<sub>SO<sub>4</sub></sub>.

## DISCUSSION

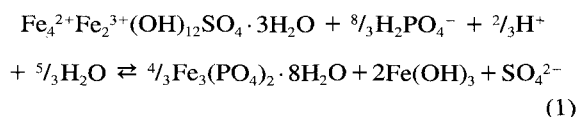
### Reaction of GR<sub>SO<sub>4</sub></sub> with Na<sub>2</sub>HPO<sub>4</sub>

For the analogues Mg-Al and Li-Al LDHs, phosphate is incorporated in the interlayers producing layer thicknesses [ $c/3 \approx d(003)$ ] in the range of 0.81 to 1.06 nm (Kosin *et al.*, 1989; Dutta and Puri, 1989; Hansen, 1995). As the thickness of the metal hydroxide layers can be assumed to be approximately constant (=0.48 nm), the variation in  $d(003)$  is attributed to differences in interlayer thicknesses. The broad range of interlayer distances for phosphate-containing LDHs provides evidence for different bonding modes for phosphate in the interlayer. Consequently, interlayer distances <1.0 nm occur when phosphate is covalently bonded to hydroxide layer metal cations (Hansen, 1995). Larger interlayer distances, ~1.0 nm, are often observed for tetrahedral oxyanions electrostatically bonded in the interlayer (*e.g.*, ClO<sub>4</sub><sup>-</sup>, SO<sub>4</sub><sup>2-</sup>). Addition of phosphate to GR<sub>SO<sub>4</sub></sub> results in a definite drop in  $d(003)$  until a stable layer thickness of 1.04 nm is reached (Figure 3). Simultaneously, an increase in [SO<sub>4</sub><sup>2-</sup>]<sub>sol</sub> occurs (Figure 4). This change demonstrated that phosphate anions exchanged with SO<sub>4</sub><sup>2-</sup> in the interlayer, and that sorbed phosphate was bonded electrostatically.

Immediately after addition of Na<sub>2</sub>HPO<sub>4</sub> to the GR<sub>SO<sub>4</sub></sub> the P<sub>solid</sub>:Fe<sub>solid</sub>-ratio of the precipitates equals 0.15 and the Fe(II)<sub>tot</sub> and Fe(II)<sub>sol</sub> concentrations were 6.50 and 0.65 mM, respectively (Figure 4). With an Fe(II):(Fe(II) + Fe(III))-ratio in GR<sub>SO<sub>4</sub></sub> of 1.5 the total concentration of Fe in GR plus solution equals (6.50 - 0.65) × 1.5 + 0.65 = 9.42 mM and the maximum content of phosphate in GR is thus 9.42 × 0.15 = 1.41 mM. Assuming that phosphate was initially involved in precipitating all the Fe(II)<sub>sol</sub> in the GR suspension as Fe(II) phosphate with an Fe:P ratio of 3:2, then 0.98 mM (1.41 - 0.65 × 2/3) of phosphate remained for sorption in GR<sub>SO<sub>4</sub></sub>. Although HPO<sub>4</sub><sup>2-</sup> is the dominating species at the pH of the suspensions (9.3), phosphate may be adsorbed in the interlayer as PO<sub>4</sub><sup>3-</sup> anion because the affinity for HPO<sub>4</sub><sup>2-</sup> will be lower due to its

lower charge (Dutta and Puri, 1989). Thus 3 × 0.98 = 2.94 mM, *i.e.*, 50% (5.85 mM), of the interlayer charge will be compensated by adsorption of PO<sub>4</sub><sup>3-</sup>. This is in reasonable agreement with the [SO<sub>4</sub><sup>2-</sup>]<sub>sol</sub> data, which indicates that 1.60 × 2 = 3.20 mM of interlayer charge became available due to SO<sub>4</sub><sup>2-</sup> desorption (Figure 4). The minor discrepancy may be caused by exposure of the suspensions to CO<sub>2(g)</sub> and subsequent interlayering of CO<sub>3</sub><sup>2-</sup>. A small peak at 0.753 nm in the XRD traces of some experiments may be attributed to GR<sub>CO<sub>3</sub></sub> (not shown). Although phosphate has exchanged with SO<sub>4</sub><sup>2-</sup>, that the selectivity for phosphate is not sufficiently high to completely exchange all interlayer SO<sub>4</sub><sup>2-</sup>.

The slowly decreasing ratio P<sub>solid</sub>:Fe<sub>solid</sub> indicates that phosphate sorbed into GR or precipitated as vivianite becomes increasingly non-extractable in 0.1 M HCl with time (Figure 4). Incomplete dissolution of vivianite in 0.1 M HCl does not fully explain this, as the increase in vivianite after 40 d (Figure 2) was not expressed in a steadily decreasing P<sub>solid</sub>:Fe<sub>solid</sub>-ratio. It is likely that the initial rapid crystallization of vivianite (0–10 d; Figure 2) can be attributed to the precipitate formed by Fe(II) in solution (Figure 4, ▲) and phosphate when Na<sub>2</sub>HPO<sub>4</sub> was added. The period from 10 to 40 d where no vivianite crystallized indicates that a lag period was needed before interlayer-phosphate combined with Fe(II) in the GR to crystallize vivianite. After day 40 more vivianite crystallizes which demonstrates that GR<sub>SO<sub>4</sub></sub> is slowly converted to vivianite in the presence of phosphate. The mechanism is probably via the phosphate-interlayered GR as an intermediate phase, indicating that GR<sub>SO<sub>4</sub></sub> may not be stable in phosphate-rich environments. Assuming that the Fe(III) in GR precipitates as ferrihydrite (probably containing phosphate) during the transformation of GR to vivianite, a rough estimate of the free energy of reaction can be computed according to the following reaction:



In this equation, “Fe(OH)<sub>3</sub>” denotes ferrihydrite. Computation of the standard free energy of reaction ( $\Delta_r G^\ominus$ ) from the thermodynamic data in Table 2 gives -187.03 kJ·mol<sup>-1</sup>. From estimated activities of SO<sub>4</sub><sup>2-</sup>, H<sub>2</sub>PO<sub>4</sub><sup>-</sup>, and H<sup>+</sup> in the anion exchange reactions of GR<sub>SO<sub>4</sub></sub> at day 60,  $\Delta_r G$  for equation (1) is calculated at -104.5 kJ·mol<sup>-1</sup>. Although the value of  $\Delta_r G^\ominus$  for GR<sub>SO<sub>4</sub></sub> is uncertain, the error in  $\Delta_r G^\ominus$  (GR<sub>SO<sub>4</sub></sub>) would need to exceed -100 kJ·mol<sup>-1</sup> for the calculated  $\Delta_r G$  value to become positive. An error of this size is unlikely. The calculations thus confirm that the transformation of GR<sub>SO<sub>4</sub></sub> to vivianite and ferrihydrite is ther-

Table 2. Standard free energies of formation ( $\Delta_r G^\ominus$ ) (25°C).

Species	$\Delta_r G^\ominus$ (kJ·mol <sup>-1</sup> )	Reference
H <sub>2</sub> O <sub>(l)</sub>	-237.13	Wagman <i>et al.</i> (1982)
H <sub>2</sub> PO <sub>4</sub> <sup>-</sup> <sub>(aq)</sub>	-1130.28	Wagman <i>et al.</i> (1982)
PO <sub>4</sub> <sup>3-</sup> <sub>(aq)</sub>	-1018.7	Wagman <i>et al.</i> (1982)
SO <sub>4</sub> <sup>2-</sup> <sub>(aq)</sub>	-744.53	Wagman <i>et al.</i> (1982)
Fe <sup>2+</sup> <sub>(aq)</sub>	-78.9	Wagman <i>et al.</i> (1982)
Fe(OH) <sub>3(s)</sub>	-699.0 <sup>1</sup>	Data cited by Fox (1988)
Fe <sub>3</sub> (PO <sub>4</sub> ) <sub>2</sub> ·8H <sub>2</sub> O <sub>(s)</sub>	-4375.3 <sup>1</sup>	Al-Borno and Tomson (1994)
Fe <sup>2+</sup> <sub>4</sub> Fe <sup>3+</sup> <sub>2</sub> (OH) <sub>12</sub> <sup>-</sup> SO <sub>4</sub> ·3H <sub>2</sub> O <sub>(s)</sub>	-4380	Hansen <i>et al.</i> (1994)

<sup>1</sup> Determined from average solubility products.

modynamically favored under the prevailing experimental conditions.

#### Reaction of P-ferrihydrite with Fe(II)

The final GR formed in this system had a  $d(003)$ -value corresponding to that of pure GR<sub>SO<sub>4</sub></sub> (Figure 1). Consequently, we conclude that the GR end-product is GR<sub>SO<sub>4</sub></sub> occurring with vivianite (Figure 7, trace d). Because phosphate is not incorporated into the interlayers of GR, this indicates that phosphate is more stable in vivianite than in GR. The GR<sub>SO<sub>4</sub></sub> is stable in the Fe(II)-rich solutions since the activity of phosphate is controlled by the solubility of vivianite. Although phosphate sorption impairs crystallization of iron(hydr)oxides (Kandori *et al.*, 1992), phosphate in this system is "scavenged" by vivianite allowing pure GR<sub>SO<sub>4</sub></sub> to form. A similar reaction is not expected in GR-silicate systems since there is no phase like vivianite which effectively "cleans" silicate from solution. This is consistent with a previous study indicating that silicate does obstruct the formation of GRs (Karim, 1986).

#### P retention under natural anoxic conditions

In anoxic environments with an excess of Fe(II) in solution, vivianite and not GR will limit the solubility of phosphate when the system reaches equilibrium. In contrast, GR systems with an excess of phosphate may temporarily sorb phosphate in GR interlayers. Also in this case, vivianite will eventually become the stable product controlling the phosphate concentration in solution. The latter system may exist naturally when phosphate-rich solutions from upper soil layers penetrate sediment layers containing GR. The exchangeability of the interlayer anion in the GR and the charge of the GR hydroxide sheets (*i.e.*, the Fe(II):Fe(III)-ratio in the GR) are likely to affect the rate and extent of phosphate sorption and the rate of GR transformation to vivianite. Most monovalent interlayer anions are more easily exchanged compared with sulphate (Miyata, 1983) and thus GRs containing monovalent anions are expected to comprise more active phos-

phate sorbents than GR<sub>SO<sub>4</sub></sub>. Thus, the hydroxyl-interlayer form of GR, which was postulated to exist in soils (Trolard *et al.*, 1997), could be a potentially strong phosphate sorbent.

In earlier studies, Fe(OH)<sub>2</sub> was suggested as a hypothetical sorbent for phosphate under anoxic conditions (Patrick and Khalid, 1974; Willett and Higgins, 1978). However, due to the higher stability of GR compared with Fe(OH)<sub>2</sub> (Arden, 1950) and the phosphate sorption capacity of GR, this phase appears to be a more likely phosphate sorbent than Fe(OH)<sub>2</sub> in anoxic soils and sediments.

## CONCLUSIONS

Green rusts may influence the retention of phosphate in Fe(II)-Fe(III)-H<sub>2</sub>O natural systems. Probably all interlayer types of GRs, not only the investigated GR<sub>SO<sub>4</sub></sub>, will react with phosphate but at different rates and to a different extent. In the presence of excess phosphate in solution, phosphate exchanges with SO<sub>4</sub><sup>2-</sup> in the interlayer of GR<sub>SO<sub>4</sub></sub> producing a GR  $d(003)$ -value of 1.044 nm. The partially phosphate-exchanged GR is slowly transformed to vivianite over a period of months. In the presence of excess Fe(II) in solution, phosphate-containing ferrihydrite reacts with Fe(II), precipitating a green amorphous Fe(II)-Fe(III)-(hydr)oxide-phosphate, which eventually is transformed to well crystallized GR<sub>SO<sub>4</sub></sub> and vivianite. Thus, whereas vivianite is the stable end-product in both systems, GR<sub>SO<sub>4</sub></sub> may be present also at equilibrium but will contain no interlayer-phosphate. Lastly, it is inferred that in natural mixed Fe(II)-Fe(III) systems, Fe(OH)<sub>2</sub> will not be stable compared to GRs and therefore will play no role with respect to retention of phosphate.

## ACKNOWLEDGMENTS

We thank H. Nancke-Krogh for experimental assistance. We are grateful to two anonymous reviewers for helpful comments.

## REFERENCES

- Al-Borno, A. and Tomson, M.B. (1994) The temperature dependence of the solubility product constant of vivianite. *Geochimica et Cosmochimica Acta*, **58**, 5373-5378.
- Allison, J.C., Brown, D.S., and Novo-Gradac, K.J. (1990) *MINTEQA2/PRODEFA2, a Geochemical Assessment Model for Environmental Systems: Version 3.00 User's Manual*. EPA-600/3-91-021, USEPA, Athens, Georgia.
- Allmann, R. (1970) Doppelschichtstrukturen mit brucitähnlichen Schichtionen [Me(II)<sub>1-x</sub>Me(III)<sub>x</sub>(OH)<sub>2</sub>]<sup>x+</sup>. *Chimia*, **24**, 99-108.
- Arden, T.V. (1950) The solubility products of ferrous and ferrous hydroxides. *Journal of the Chemical Society*, 882-885.
- Bernal, J.D., Dasgupta, D.T., and Mackay, A.L. (1959) The oxides and hydroxides of iron and their structural interrelationships. *Clay Minerals Bulletin*, **4**, 15-30.
- Brindley, G.W. and Bish, D.L. (1976) GR: A pyroaurite type structure. *Nature*, **263**, 353.

- Dutta, P.K. and Puri, M. (1989) Anion exchange in lithium aluminate hydroxides. *Journal of Physical Chemistry*, **96**, 376–381.
- Fadrus, H. and Maly, J. (1975) Suppression of iron(III) interference in the determination of iron(II) in water by the 1,10-phenanthroline method. *Analyst*, **100**, 549–554.
- Feitknecht, W. and Keller, G. (1950) Über die dunkelgrünen Hydroxyverbindungen des Eisens. *Zeitschrift für anorganische Chemie*, **262**, 61–68.
- Fox, L.E. (1988) The solubility of colloidal ferric hydroxide and its relevance to iron concentrations in river water. *Geochimica et Cosmochimica Acta*, **52**, 771–777.
- Hansen, H.C.B. (1989) Composition, stabilization, and light absorption of Fe(II)Fe(III) hydroxy-carbonate ('Green Rust'). *Clay Minerals*, **24**, 663–669.
- Hansen, H.C.B. (1994) *TITRA—A MS Windows 3.x program for communication between Metrohm pH-meters/dosimeters and a PC via RS-232*. Technical Report, Chemistry Department, The Royal Veterinary and Agricultural University, Copenhagen, 83 pp. (in Danish).
- Hansen, H.C.B. (1995) Interlayer-bonding of orthophosphate and orthosilicate in layered magnesium-aluminium hydroxide (Hydrotalcite). In *Proceedings of the 10th International Clay Conference Adelaide, Australia*, 201–206.
- Hansen, H.C.B., Borggaard, O.K., and Sørensen, J. (1994) Evaluation of the free energy of formation of iron(II)iron(III)-hydroxide-sulphate (Green Rust) and its reduction of nitrite. *Geochimica et Cosmochimica Acta*, **58**, 2599–2608.
- Hansen, H.C.B., Koch, C.B., Nancke-Krogsh, H., Borggaard, O.K., and Sørensen, J. (1996) Abiotic nitrate reduction to ammonium: Key role of green rust. *Environmental Science and Technology*, **30**, 2053–2056.
- Holford, I.C.R. and Patrick, W.H., Jr. (1979) Effects of reduction and pH changes on phosphate sorption and mobility in an acid soil. *Soil Science Society of America Journal*, **43**, 292–297.
- Kandori, K., Uchida, S., Kataoka, S., and Ishihawa, T. (1992) Effects of silicate and phosphate on the formation of ferric oxide hydroxide particles. *Journal of Materials Science*, **26**, 3313–3319.
- Karim, Z. (1986) Formation of ferrihydrite by inhibition of green rust structures in the presence of silicon. *Soil Science Society of America Journal*, **50**, 247–250.
- Koch, C.B. and Hansen, H.C.B. (1997) Reduction of nitrate to ammonium by sulphate green rust. *Advances in Geoecology*, **30**, 373–393.
- Kosin, J.A., Preston, B.W., and Wallace, D.N. (1989) *Modified synthetic hydrotalcite*. US Patent 4.883.533.
- Lovley, D.R. (1987) Organic matter mineralization with the reduction of ferric iron: A review. *Geomicrobiology Journal*, **5**, 375–399.
- Lovley, D.R. (1991) Dissimilatory Fe(III) and Mn(IV) reduction. *Microbiological Reviews*, **55**, 259–287.
- Miyata, S. (1983) Anion-exchange properties of hydrotalcite-like compounds. *Clays and Clay Minerals*, **31**, 305–311.
- Nriagu, J.O. and Dell, C.I. (1974) Diagenetic formation of iron phosphates in recent lake sediments. *American Mineralogist*, **59**, 934–946.
- Patrick, W.H., Jr. and Khalid, R.A. (1974) Phosphate release and sorption by soils and sediments: Effect of aerobic and anaerobic conditions. *Science*, **186**, 53–55.
- Ponnamperuma, F.N. (1972) The chemistry of submerged soils. *Advances in Agronomy*, **24**, 29–96.
- Reardon, E.J. and Della Vale, S. (1997) Anion sequestering by the formation of anionic clays: Lime treatment of fly ash slurries. *Environmental Science and Technology*, **31**, 1218–1223.
- Shin, H.S., Kim, M.J., Nam, S.Y., and Moon, H.C. (1996) Phosphorus removal by hydrotalcite-like compounds (HTLcs). *Water Science and Technology*, **34**, 161–168.
- Siemens (1997) *Diffraction Plus Evaluation Program. User's Guide*. Siemens, Karlsruhe, 128 pp.
- Szilas, C.P., Borggaard, O.K., Hansen, H.C.B., and Rauer, J. (1997) Potential iron and phosphate mobilization during flooding of soil material. *Water, Air and Soil Pollution*, **106**, 97–109.
- Tamaura, Y., Saturno, M., Yamada, K., and Katsura, T. (1984a) The transformation of  $\gamma$ -FeO(OH) to Fe<sub>3</sub>O<sub>4</sub> and green rust II in an aqueous solution. *Bulletin of the Chemical Society of Japan*, **57**, 2417–2421.
- Tamaura, Y., Yoshida, T., and Katsura, T. (1984b) The synthesis of green rust II (Fe<sup>II</sup>-Fe<sup>III</sup>) and its spontaneous transformation into Fe<sub>3</sub>O<sub>4</sub>. *Bulletin of the Chemical Society of Japan*, **57**, 2411–2416.
- Taylor, R.M. (1980) Formation and properties of Fe(II)Fe(III) hydroxycarbonate and its possible significance in soil formation. *Clay Minerals*, **15**, 369–382.
- Taylor, R.M. and McKenzie, R.M. (1980) The influence of aluminum on iron oxides. VI. The formation of Fe(II)-Al(III) hydroxy-chlorides, -sulfates, and -carbonates as new members of the pyroaurite group and their significance in soils. *Clays and Clay Minerals*, **28**, 179–187.
- Tecator (1983) Determination of total phosphorus in water by flow injection analysis. Application Note, ASN 60-02/03, Höganäs, Sweden.
- Trolard, F., Génin, J.M.R., Abdelmoula, M., Bourrié, G., Humbert, B., and Herbillon, A. (1997) Identification of a green rust mineral in a reductomorphic soil by Mössbauer and Raman spectroscopies. *Geochimica et Cosmochimica Acta*, **61**, 1107–1111.
- Wagman, D.D., Evans, W.H., Parker, V.B., Schumm, H., Halow, I., Bailey, S.M., Churney, K.L., and Nuttall, R.L. (1982) The NBS tables of chemical thermodynamic properties. Selected values for inorganic and C<sub>1</sub> and C<sub>2</sub> organic substances in SI units. *Journal of Physical and Chemical Reference Data*, **11**, (Supplement 2).
- Westergaard, B., Hansen, H.C.B., and Borggaard, O.K. (1998) Determination of anions in soil solutions by capillary zone electrophoresis. *Analyst*, **123**, 721–724.
- Vins, J., Subrt, J., Zapletal, V., and Hanousek, F. (1987) Preparation and properties of green rust type substances. *Collection of the Czechoslovak Chemical Communications*, **52**, 93–102.
- Willett, I.R. (1985) The reductive dissolution of phosphated ferrihydrite and strengite. *Australian Journal of Soil Research*, **23**, 237–244.
- Willett, I.R. (1986) Phosphorus dynamics in relation to redox processes in flooded soils. In *Transactions of the 13th Congress of the International Soil Science Society, Hamburg*. Volume VI, 748–755.
- Willett, I.R. (1989) Causes and prediction of changes in extractable phosphorus during flooding. *Australian Journal of Soil Research*, **27**, 45–54.
- Willett, I.R. and Higgins, M.L. (1978) Phosphate sorption by reduced and reoxidized rice soils. *Australian Journal of Soil Research*, **16**, 319–326.
- Williams, J.D.H., Syers, J.K., Shukla, S.S., Harris, R.F., and Armstrong, D.E. (1971) Levels of inorganic and total phosphorus in lake sediments as related to other sediment parameters. *Environmental Science and Technology*, **5**, 1113–1120.

(Received 26 January 1998; accepted 15 October 1998; Ms. 98-017)